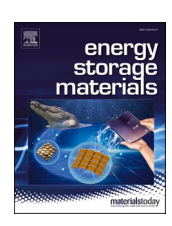
ELSEVIER

Contents lists available at ScienceDirect

Energy Storage Materials

journal homepage: www.elsevier.com/locate/ensm





Modulation and quantitative study of conformal electrode-electrolyte interfacial chemistry toward high-energy-density $\text{LiNi}_{0.6}\text{Co}_{0.2}\text{Mn}_{0.2}\text{O}_2\|\text{SiO-C}$ pouch cells

Weimin Zhao a,1 , Guorui Zheng b,1 , Yuchen Ji b , Chengxin Peng c , Fucheng Ren d , Ming Liu e , Feng Pan b,* , Yong Yang f,*

- ^a College of Chemical Engineering and Safety, Binzhou University, Binzhou 256600, China
- ^b School of Advanced Materials, Peking University Shenzhen Graduate School, Shenzhen 518055, China
- ^c School of Materials Science and Engineering, University of Shanghai for Science and Technology, Shanghai 200093, China
- ^d School of Energy Research, Xiamen University, Xiamen 361005, China
- ^e Shenzhen All-Solid-State Lithium Battery Electrolyte Engineering Research Center, Tsinghua Shenzhen International Graduate School, Tsinghua University, Institute of Materials Research (IMR), Shenzhen 518055, China
- f State Key Laboratory for Physical Chemistry of Solid Surfaces, Collaborative Innovation Center of Chemistry for Energy Materials, Department of Chemistry, College of Chemistry and Chemical Engineering, Xiamen University, Xiamen 361005, China

ARTICLE INFO

Keywords: Electrolyte additive Interface film Lithium difluorobis(oxalato) phosphate Pouch cell

ABSTRACT

High-nickel layered ternary cathode coupling with Si-based anode is one of the most promising strategies to realize high-energy-density batteries for power electric vehicles. However, undesired interfacial instability on both sides of cathode and anode causes continuous parasitic reactions and phase transformations, and results in fast degradation of the batteries. To address this issue, herein, in-situ reliable, compact and ionically conductive interface films are constructed effectively on both LiNi_{0.6}Co_{0.2}Mn_{0.2}O₂ (NMC622) cathode and SiO-C anode simultaneously by simply using a multifunctional additive, lithium difluorobis(oxalato) phosphate (LiDFBOP), due to its preferential redox reactivity then efficiently influencing the subsequent electrochemical behaviors of bulk electrolyte. These films shield the electrodes against the electrolyte attack, thus enabling long-term cycling stability and enhancing Coulombic efficiency of NMC622/SiO-C pouch cells. In addition, the highly Li-ionically conductive interphases also promote the electrode kinetics, which ensure the excellent rate capability as well as low temperature performance. The underlying interface formation mechanisms in term of specific consumption amount of additive on each electrode simultaneously are quantitatively studied by combining several complementary advanced characterizations techniques such as IC, TOF-SIMS, XPS and HRTEM etc., which not only benefit to predict the optimal addition content for cost-effective electrolyte in the actual conditions, but also validate that abundant Li-containing fluorinated inorganics and organic species regulate the microstructure and the composition of interface films, leading to enhanced ionic conductivity and intensified structure integrity, then finally contributing to the improved electrochemical performance of full pouch cells. New and in-depth insight in additive-involved interface reactions provides new opportunities for the design of rational surface films to realize high-energy batteries.

1. Introduction

Lithium (Li)-ion (Li⁺) batteries (LIBs) with high energy density and safety are urgently required for implementation in the field of electric vehicles, which depends on high specific capacity delivery with high

discharge voltage output [1,2]. Traditional commercial LIBs comprising of graphite anode and LiCoO₂ cathode have almost reached their upper limit in energy density due to the unsatisfactory capacity [3]. Therefore, it is critical to develop next-generation electrode materials to break through this bottleneck [4,5]. As for cathodes, due to the synergy

E-mail addresses: panfeng@pkusz.edu.cn (F. Pan), yyang@xmu.edu.cn (Y. Yang).

^{*} Corresponding authors.

¹ These authors contributed equally to this work.

between transition metal ions, layered ternary composite materials LiNi_{1-x-v}Co_xMn_vO₂ became most promising in recent years [6,7]. Among them, the cathodes with enhanced Ni content perform higher capacity delivery [8-10]. However, because the radius of Ni is similar to Li, the increase of Ni content might cause the dislocation and mixed arrangement between Ni and Li, leading to high-concentrated Ni in Li layer [11]. This would result in difficulties in Li diffusion when cycling and final poor cycling stability and rate capability and even structural deterioration. Besides, interfacial instability could trigger continuous side reaction and accelerate decay of cathode especially when cycled in high cut-off charge voltage [12]. Therefore, a good quality interface layer is necessary, which not only protects the cathode from being attacked by electrolyte, but also play a role in helping stabilize structural integrity of cathode and preventing dissolution of transition metal ions [13]. As for anodes, due to their high capacity and low discharge potential, Si-C composite materials are expected to be widely used commercially for realizing higher energy density and safer LIBs in the short term [14,15]. However, severe interfacial instability associated with continuous side reactions and infinite volume changes still remians to be solved [16,17]. Therefore, an interface layer with highly mechanical properties, electrochemical stability and improved Li⁺ conductivity is needed for a better cycling performance.

From the above, it follows that constructing a more stable and ionically conductive interface film on both cathode and anode simultaneously is vital to perform a high-energy battery with high-capacity electrode materials. Of many strategies, electrolyte modification such as introducing a multifunctional electrolyte add9itive to the nonaqueous liquid electrolyte shows significant advantages being low cost, easy to implement and allowing better compatibility for practical batteries [18, 19]. However, most of interface film-forming organic electrolyte additives reported which focused on stabilizing electrolytes at cathode surfaces might be detrimental to the performance of the paired anodes and vice versa [20,21]. On the other hand, compared to organic additives, Li salt-type electrolyte additives could provide Li⁺ to be incorporated into the interface films, leading to their decreasing interface impedance, enhancing mechanical and electrochemical stability, and even improved low-temperature properties [22-24]. Therefore, in recent years, many different kinds of them have been proposed and extensively studied, such as lithium hexafluorophosphate (LiPF₆) [25], lithium difluorophosphate (LiDFP) [26,27], and lithium bis(oxalato) borate (LiBOB) [28,29]. Among them, LiBOB has shown its capability in protecting surfaces either on cathode or on anode respectively. It can be reduced at around 1.2 V (versus Li metal) and contribute to form a stable interface layer on graphite, which effectively inhibits co-intercalation of solvent even in the pure propylene carbonate solvent. Also, it was confirmed to oxidize on cathode surface, forming polyboric acid or oxalic acid compounds in the interface film to prevent the corrosion of the cathode by electrolyte. However, its poor solubility and consequent high-resistance interface films severely limit its commercial applications. Lithium difluorobis(oxalato) phosphate (LiDFBOP), having the same oxalate anions as LiBOB, a new developed salt-type electrolyte additive derived from the structural replace towards LiPF₆, was confirmed to be beneficial to stabilize both cathode and anode [30-32]. However, based on constructing a next-generation high-energy batteries, there is rarely reported that a systematic research towards its participation in forming solid electrolyte interfaces (SEIs) with desirable structures for Si anodes and cathode electrolyte interfaces (CEIs) for Ni-rich cathodes in full cells; furthermore, it has been lacking a novel approach proposed to quantify and differentiate the necessary sacrifice of additive on both anode and cathode simultaneously in real full cells to understand the interfacial behaviors and specific consumption process of additives associated with regulating the subsequent formation mechanisms of interface films on each electrode and their contributions to the improved performances.

Therefore, in this work, we report an emerging multifunctional LiDFBOP additive in stabilizing the cathode and anode interfaces

simultaneously based on high-energy-density LiNi_{0.6}Co_{0.2}Mn_{0.2}O₂ (NMC622)/SiO-C full cells, demonstrating their improved electrochemical performance. The theoretical calculations and experimental electrochemical measurements are combined to understand the effects of the decomposition of additive on subsequent interfacial electrochemical behaviors of electrolyte. A new method is introduced by optimizing charge/discharge strategies with ion chromatography (IC) measurements to quantitatively analyze the specific consumption amount of additive on each electrode interface respectively during cycling and discuss the possibility in predicting the optimal usage amount of additive in the actual conditions for designing an ideal and cost-saving electrolyte. By conducting complementary spectroscopic characterizations techniques, the underlying formation mechanisms of interface films affected by additive on each SiO-C and Ni-rich electrode and their contributions to the improved electrochemical performance of batteries are further discussed.

2. Experimental section/methods

2.1. Preparation of Electrodes for pouch cells

2500 mA h LiNi_{0.6}Mn_{0.2}Co_{0.2}O₂ (NMC622)/SiO-artificial graphite materials (SiO-C) pouch cells (without electrolyte) with the type of 50*60*100 mm were manufactured by Tianjin JEVE Power Industry Co., Ltd technology (Tianjin, China), which were assembled by using doublefaced active material-coated positive and negative electrode plates. The cathode composite electrode consists of the mixture of NMC622 materials (Xiamen Tungsten Co. Ltd., China), carbon black, and polyvinylidene difluoride (PVDF) in a weight ratio of 96:1.5:2.5 coated onto an Al current collector. The anode composite electrode contains the mixture of SiO-C (BTR Battery Materials Co., Ltd., Shenzhen, China), Super-P, carboxymethyl cellulose (CMC) and styrene butadiene rubber (SBR) in a weight ratio of 95:1:1.5:2.5 coated onto Cu current collector. The loading mass of active material on each NMC622 cathode or SiO-C anode composite electrodes is 339 g m⁻² or 161 g m⁻², respectively, leading to a N/P ratio of 1.14. The other two kinds of NMC622/Li and SiO-C/Li batteries for measurements and subsequent characterizations are assembled based on the type of half coin cells instead of pouch cells, which mainly aimed for evaluating the effects of additive on the filmforming potential and electrochemical behavior of electrolyte on individual cathode or anode separately. The half coin cells used the circular electrode plates tailored from what employed in pouch cells above mentioned.

2.2. Preparation of electrolytes

 $1~M~LiPF_6$ was dissolved in mixture solvents of ethylene carbonate (EC)/ethyl methyl carbonate (EMC) (3:7, wt.%) denoted as baseline electrolyte, and lithium difluorobis(oxalato) phosphate (LiDFBOP) as an electrolyte additive, was obtained from CHUNBO Co., Ltd (Busan, South Korea). Lithium bis(oxalato) borate (LiBOB, Tianjin Jin-Niu power sources Co., Ltd) was chosen as an electrolyte additive for comparison in part of the experiments. For testing, the injection amount of electrolyte into each pouche cell is controlled at about 7.0 $\pm~0.05~\rm g.$

2.3. Electrochemical measurements

Linear sweep voltammetry (LSV) was performed on a CHI660E instrumental electrochemical station (Chinstruments, China) using a three-electrode configuration with platinum electrode as the working electrode and lithium foil as the counter and pseudo reference electrodes. The LSV measurements were conducted by setting the voltage range between 3.0 and 6.5 V (vs. Li^+/Li) with a scanning rate of 0.1 mV s⁻¹. Cyclic voltammetry (CV) experiments were conducted at a scan rate of 0.1 mV s⁻¹ and a potential range of 0 V–2.5 V (vs. Li^+/Li) on a four-channel multifunctional electrochemical work station (PARSTAT MC).

The charging/discharging behaviors of the batteries were tested using a battery charger test (CT-3008W, Neware, China). The formation cycle for the pouch cell was separated into three stages including the various current rate of C/10, C/2 for charging and C/5 for discharging at a voltage range of 3.0-4.3 V. Afterwards, the cells were transferred into the glove box, opened to release any gas generated during the formation cycle and then sealed again for long-term cycling test. The current for long-term cycling is 2500 mA (1C) by a constant current/constant voltage mode within a voltage range of 3.0-4.3 V at 25 °C. For evaluating the low-temperature properties, the pouch cells were discharged to 2.5 V at a constant current of 0.2C after stored for 12 h under 100% state of charge (SOC) at -20°C. The electrochemical impedance spectroscopy (EIS) analysis was tested on a frequency response analyzer (FRA, Solartron
1455A, Solartron Group, UK) with an amplitude potential of
 $10\,$ mV and frequency range between 0.04 Hz and 100 kHz. All the cells were conducted at a nearly half SOC condition after a potentiostatic equilibration step at 4.0 V.

2.4. Materials characterizations

For the structure and composition characterizations, the cycled SiO-C and NMC622 electrodes were retrieved and washed three times with anhydrous EMC to remove residual salts and solvents, then evacuated overnight in the glove box (Braun company, Germany, $H_2O < 0.1$ ppm, $O_2 < 0.1$ ppm) at room temperature. X-ray diffraction (XRD) patterns of the cycled NMC622 cathodes were obtained by a Rigaku Ultima IV with Cu Ka radiation. Field emission scanning electron microscopy (SEM, HITACHI S-4800, Japan) coupled with an energy dispersive X-ray spectrometer (EDS) was supplied to characterize the morphologies, structures and surface elemental distribution of cycled electrodes. Transmission electron microscopy (TEM) was conducted by operating at 200 kV on a Tecnai F20 (Philip-FEI, Netherlands) apparatus. X-ray photoelectron spectroscopy (XPS) was acquired under monochromatic Al K α radiation (h ν = 1486.6 eV) with a Quantum 2000 ESCA spectrometer (Physical Electronics, USA) equipped at 23.2 W and in a vacuum value less than 10^{-8} Torr. In details, the cycled cells were dismantled in a glove box under Argon atmosphere and the electrodes inside were then washed as mentioned above and transferred into the special XPS vacuum chamber. The universal contamination of C-H bond at 284.8 eV was used as a reference for the final adjustment of the energy scale in the spectra. The quantitative and qualitative researches of inorganic lithium salt components at different SOC were conducted by ion chromatography (IC) experiments on a Thermo Fisher Scientific Ion chromatography (Aquion ICS-2100). The specific operation process of IC is as below: Firstly, the mixed solution of 1.8 mM Na₂CO₃ and 1.8 mM NaHCO₃ with 20 vol.% acetonitrile was prepared as leacheate at a flow rate of 1.0 mL min⁻¹ and 20 mM H₂SO₄ solution was used as regenerated liquid at a same flow rate of 1.0 mL min⁻¹. Then the pump flow rate was set to 2 mL min⁻¹, and the temperature of the cylinder was 35 °C. When the system pressure rose to 1000 kPa, the current was set to 5 mA and the suppressor was opened. The system was balanced for about 30 min, and the detection sample diluted 2000 times was processed on the IC machine for testing. A time-of-flight secondary ion mass spectrum (TOF-SIMS) was measured on an ION-TOF GmbH TOF-SIMS 5-100 spectrometer. The analysis chamber was maintained in ultrahigh vacuum at a pressure below 2×10^{-9} mbar and a 500 eV Cs $^+$ ion beam (maintaining sputtering rate of 0.03 nm s⁻¹) was applied for sputtering the cycled NMC622 and SiO-C electrodes for depth profiling. The typical sputtering area was 100×100 um. All the detected secondary ions of interest had a mass resolution of > 12,000 and a depth resolution of < 1

2.5. Computational methods

Density functional theory (DFT) was employed to investigate the reduction and oxidation processes of the additive molecule. The specific

structures were fully optimized by the B3PW91 method with the basis set of 6-311++G (d, p). The polarized continuum model (PCM) as implemented in Gaussian09 was used to describe the implicit solvent effect on the reduction and oxidation processes of the additives. Dielectric constant of EC (89.6) was used for all PCM calculations.

3. Results and discussion

3.1. Effect of LiDFBOP additive on electrochemical behaviors of electrolyte

To evaluate the effect of LiDFBOP additive on the physicochemical properties of electrolytes, we measured and compared the water content, Li⁺ conductivity and viscosity of different electrolytes. As shown in Table S1, the water contents of all the electrolytes meet the requirement for direct application in preparing batteries for kinds of electrochemical measurements without further treatment; when adding LiDFBOP to the baseline electrolyte, there is less decrease in the Li⁺ conductivity with less increase in the viscosity than the electrolyte with LiBOB, which indicates the LiDFBOP additive is a more potential candidate for realizing a better rate performance battery with less sensitive to environmental temperature. Then IC measurement was used to analyze the chemical stability of the electrolyte with LiDFBOP at elevated temperature. As shown in Fig. S1, we compared the chemical compositions of the electrolyte before and after stored at 60°C for different time. Evidently, there is almost no change detected in the electrolyte with LiDFBOP throughout, indicating its better high-temperature chemical stability.

To construct a better interface film, film-forming additive is used to be introduced as a sacrificial agent and expected to preferentially decompose before the bulk electrolyte, thereby affecting the subsequent reactions occurring on the electrode interfaces and improving the electrochemical performance of interface films. Therefore, it is important to understand the reactivity of all electrolyte components involved theoretically and experimentally. Firstly, as presented in Fig. 1a, we calculated and compared the highest occupied molecular orbital (HOMO), the lowest unoccupied molecular orbital (LUMO) and the bond-dissociation energies of LiDFBOP in comparison with the EC and EMC solvents, LiPF₆ salt and another additive LiBOB. As summarized in Table S2, the LiDF-BOP additive exhibits higher HOMO energy and lower LUMO energy than solvents, Li salt and even LiBOB additive, suggesting its possibility in preferential oxidation on the cathode interfaces and reduction on the anode interfaces respectively as concluded in Fig. 1b. This may help form the original interfaces on the electrodes and change their electrochemical behaviors. Besides, the LiDFBOP additive shows the lowest dissociation energy among all the Li salts used, suggesting its potentially better solubility in the carbonic ester solvents. Then we conducted the linear sweep voltammetry (LSV) and cyclic voltammetry (CV) for getting the electrochemical stability window of different electrolytes to further verify the reactivity of LiDFBOP and analyze its effects on the electrochemical behaviors of modified electrolytes. Comparing the LSV curves displayed in Fig. 1c, for the baseline electrolyte, there is no evident oxidation peak of electrolyte below 6.0 V (versus Li metal reference), after which a significant oxidation peak appears, indicating that the baseline electrolyte starts to decompose dramatically. However, when adding the LiDFBOP or LiBOB additive to the baseline electrolyte, small oxidation peaks are found below 6.0 V, which originate from the preferential decomposition of oxalate-containing anions from additives before the decomposition of bulk electrolyte [33]. In order to further elucidate the redox reaction mechanism of LiDFBOP, we calculated its charge distribution (Fig. S2a) and orbital distributions of HOMO and LUMO (Fig. S2b) under both the oxidation and reduction states by density functional theory (DFT). The result shows that the frontier orbitals are distributed on the oxalate, which is consistent with the simulation of charge distribution, indicating that the oxalate functional group of LiDFBOP is the most reactive in both the oxidation and

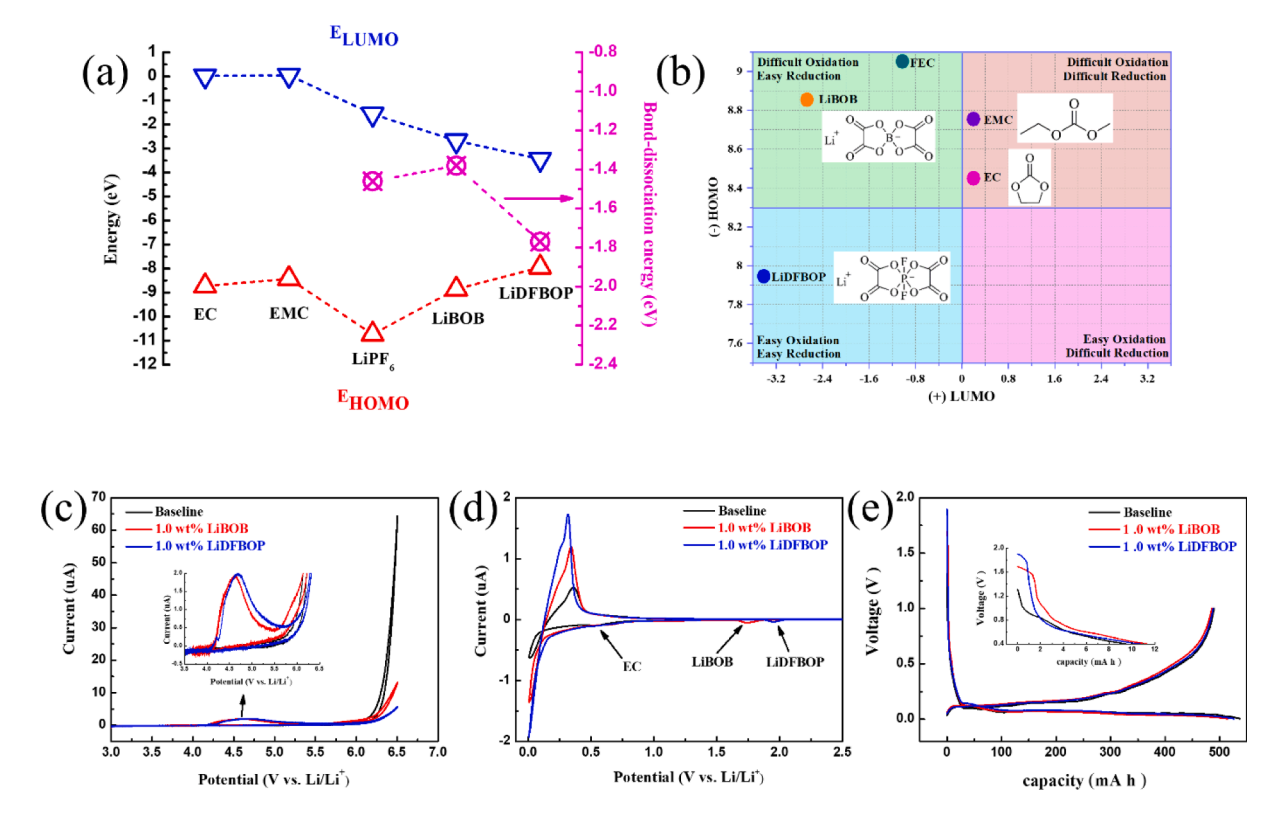


Fig. 1. Effect of additives on electrochemical behaviors of electrolytes. (a) The calculated HOMO, LUMO and bond-dissociation energies of solvents, Li salt and electrolyte additives. (b) The comparisons of redox reactivity of different common electrolytic components. (c) LSV curves of different electrolytes on platinum electrodes at a scan rate of 0.1 mV s⁻¹. (d) CV curves of SiO-C/Li half cells using baseline and additive-containing electrolytes at a scan rate of 0.1 mV s⁻¹ and a potential range of 0 V–2.5 V (vs. Li $^+$ /Li) for the first cycle. (e) Galvanostatic voltage profiles of SiO-C/Li half cells using baseline and additive-containing electrolytes at a current rate of 0.1C and a potential range of 5 mV-1 V for the first discharge/charge cycle.

reduction processes and is prone to bond-breaking. Interestingly, the initial oxidation potential of 4.0 V from LiDFBOP is lower than that of 4.25 V from LiBOB, which is in accordance with the results from theoretical calculation that LiDFBOP is easier to oxidize than LiBOB. Furthermore, it is reasonable to draw a preliminary conclusion that the early sacrifice of LiDFBOP or LiBOB additive is helpful to postpone and inhibit the oxidation decomposition of baseline electrolyte, contributing to the overall improved stability of the modified electrolytes against electrochemical oxidation. From the CV curves shown in Fig. 1d, the stability of electrolytes with different additives against electrochemical reduction is discussed. For the baseline electrolyte, there appears an irreversible reduction peak centered at about 0.60 V, which can be ascribed to the reduction decomposition of EC solvent [18]. This peak can be suppressed by adding LiBOB or LiDFBOP additive to the baseline electrolyte. For the electrolyte with 1.0 wt.% LiBOB, a new small irreversible peak centered at about 1.70 V appears, which can be assigned to the reduction decomposition of LiBOB additive. On adding 1 wt.% LiDFBOP to the baseline electrolyte, a new irreversible reduction peak of LiDFBOP additive centered at higher potential of about 1.95 V is identified, again demonstrating its easier reduction reactivity. The preferential reduction decomposition of both kinds of additives helps suppress subsequent excessive decomposition of EC solvent. Besides, an improved lithiation/delithiation dynamics of SiO-C anode can be seen when cycled in the additive-added electrolyte, especially for the LiDFBOP additive, reflecting a better interface layer formed on the anode due to the effect of the LiDFBOP additive. As exhibited in Fig. 1e, we also compared the first-cycle galvanostatic voltage profiles of SiO-C/Li half cells to check the effects of additives on electrochemical behaviors based on real discharge/charge. The same conclusion can be obtained that LiDFBOP additive is easier to reduce at about 1.90 V than LiBOB at about 1.63 V and any other components in the electrolyte. Based on these

observations above, LiDFBOP could be a rational candidate for constructing stable interfaces on both cathode and anode simultaneously to realize high-performance and high-energy-density NMC622/SiO-C full cells.

3.2. LiDFBOP additive in electrolyte enabling NMC622/SiO-C pouch cells

To understand the impact of additives on electrochemical cycling performance, NMC622/SiO-C pouch cells were assembled and galvanostatic measurements were conducted. Fig. S3a compares the preformation voltage profiles of pouch cells with different additives acquired by setting the current density of 0.1C (1C = 2500 mA) and charging cutoff voltage to 4.0 V. As displayed in the detailed inset, there appear evident charging platforms at about 1.80 V (vs. SiO-C anode) and 2.0 V for the pouch cells with LiDFBOP and LiBOB additive respectively, while almost nothing found for the pouch cell using the baseline electrolyte. This can be ascribed to the reduction decomposition of additives on the SiO-C anode interfaces, which is responsible to the subsequent decreasing voltage polarization on charging period and finally leading to higher charging capacity during the formation stage. Then the current densities of 0.5C and 0.2C were applied during charging and discharging process respectively to finalize formation cycle at a voltage range of 3.0-4.3 V as shown in Fig. S3b-c. Related charging and discharging data are summarized in Table S3, compared to the baseline electrolyte, there is more capacity delivery at both charging and discharging process while a little bit lower Coulombic efficiency (CE) output for the electrolytes with additives, suggesting that during the formation cycle the additives used were involved into the formation of interface films resulting in the increase of irreversible capacity. However, these films show better Li⁺ dynamic, thereby leading to the decreasing voltage hysteresis and the increasing capacity during both charging and discharging process. This might influence the battery on the performance of long-term cycling and rate capability, even low-temperature properties.

Herein, Fig. 2a-b shows long-term cycling stability and CE of the NMC622/SiO-C pouch cells using different electrolytes with different additives at a constant current density of 1C and a voltage range of 3.0-4.3 V. After 400 cycles, the cell using baseline electrolyte has a capacity retention of only 76.8% with a lower average CE of only 99.7%, showing its poor cycling stability. When LiBOB was added into the baseline electrolyte, the capacity retention is enhanced up to 84.2% with an improved average CE of 99.8%. Furthermore, there is a higher capacity retention of 87.2% with an average CE exceeding 99.8% when cycling the cell using the electrolyte with LiDFBOP additive, indicating its best cycling performance deriving from the stable interfaces formed on both electrodes.

To study the electrochemical properties of the interface layer, electrochemical impedance spectra (EIS) of SiO-C/NMC622 pouch cells with different electrolytes were recorded with charging to 4.0 V during the formation cycle. As shown in Fig. S4, all Nyquist plots can be divided into three parts by the range of frequency. A high-frequency depressed semicircle is ascribed to Li⁺ migration through the passivating layer on interface; an intermediate frequency dispersion characteristic indicates a charge transfer associated with Li⁺ migration at the electrode interface; the very low-frequency inclined tail represents the Li⁺ diffusion process [34]. Thus, the diversity of the impedance curves derives from the nature of the interface films and the kinetic characteristics of Li⁺. As expected, the addition of LiDFBOP furthest decreases the resistance of the interface film leading to promoted Li⁺ dynamics, which is beneficial to improve the rate capability of batteries. This phenomenon suggests LiDFBOP additive participates in and regulate the formation of interface layer with better Li⁺ dynamic behaviors. As shown in Fig. 2c, the pouch cell using the electrolyte with LiDFBOP additive shows better rate performance at various current densities. Even at a high rate of 5C, there still exhibits a capacity of almost 1000 mA h. The results further confirm that the addition of LiDFBOP to the baseline electrolyte have a good combination of electrochemical activity and cycle stability.

The temperature for cycling is one of the key factors to influence the electrochemical performance of batteries. Low temperature could increase the viscosity, limit solubility of Li salt and decrease Li⁺ conductivity of the electrolyte, leading to enhanced resistance and polarization of batteries. This would cause several issues such as low discharge voltage, limited capacity delivery and the precipitation of lithium metal on the anode [35,36]. Therefore, it is urgent to improve the performance of batteries charging and discharging at low temperature to expand their practicability. Herein, as shown in Fig. 2d, we also tested the pouch cells at -20°C to understand the effects of LiDFBOP additive on their low-temperature properties. In comparison with cycling at room temperature, the median discharge voltage of the pouch cell with baseline electrolyte cycled at low temperature decreases from 3.7 V to 3.1 V, indicating severe polarization leading to only 800 mA h capacity delivery, which is caused by slow Li⁺ diffusion due to the increasing viscosity of electrolyte and interfacial resistance. Therefore, constructing a highly conductive and stable interface film is important for improved low-temperature properties. It is obvious that with the addition of LiDFBOP to the baseline electrolyte, the median discharge voltage significantly increases up to 3.2 V and the capacity delivery is almost 1000 mA h, while the addition of LiBOB just shows a limited improvement. Therefore, as shown in Fig. S5, more stable long-term cycling with higher capacity delivery can be achieved when cycling the pouch cell with LiDFBOP additive at -20°C. These observations again suggest that LiDFBOP additive is involved to form a better interface film even at such

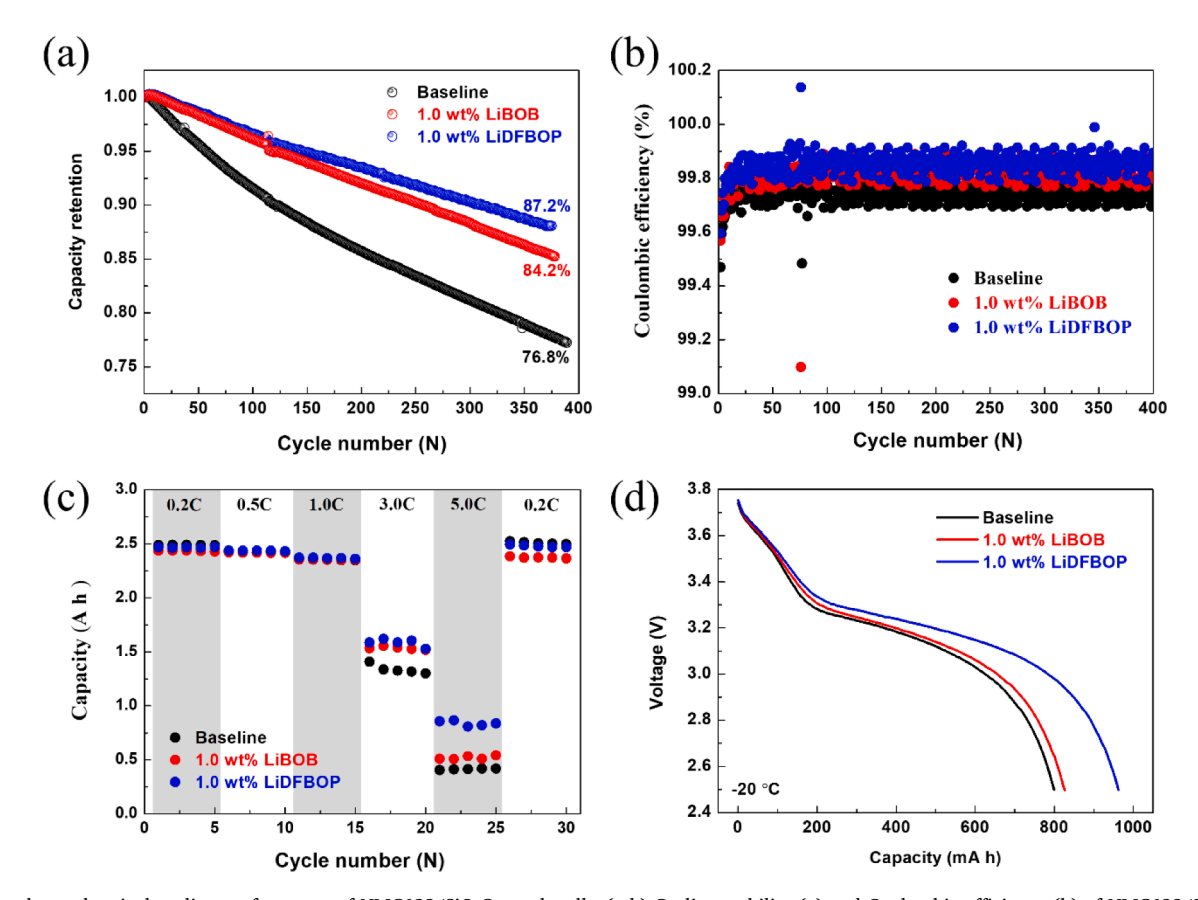


Fig. 2. The electrochemical cycling performance of NMC622/SiO-C pouch cells. (a-b) Cycling stability (a) and Coulombic efficiency (b) of NMC622/SiO-C pouch cells using different electrolytes at a current density of 1C and a potential range of 3.0–4.3 V. (c) Rate capability of NMC622/SiO-C pouch cells using different electrolytes at various current densities. (d) Discharging voltage profiles of NMC622/SiO-C pouch cells using different electrolytes with a current rate of 0.2C at low temperature of -20 °C.

a low temperature.

3.3. Characterizations of LiDFBOP additive-involved film-forming mechanism on both cathode and anode interfaces

As discussed above, the improved interfaces stability and their better electrochemical properties on both cathode and anode surfaces dependent on the LiDFBOP additive used should be the main reason leading to better electrochemical performance of the NMC622/SiO-C pouch cells. Therefore, it is necessary to understand the related LiDFBOP additiveinvolved film-forming mechanisms on both cathode and anode interfaces simultaneously. So far, there has already reported many researches focusing on studying working mechanism of additive either for cathodes or anodes, most examples of which includes various organic additives such as fluoroethylene carbonate (FEC), vinylene carbonate (VC), and propane sultone (PS) [37-40]. However, based on the new-generation representative NMC622/SiO-C pouch cells, it has been lacking to reveal the redox nature and decomposition dynamics of multifunctional salt-type additive like LiDFBOP which modifies both positive and negative electrodes interfaces simultaneously. Besides, to the best of our knowledge, there is no research focusing on discussing the precise usage amount of electrolyte additive and its respective consumption amount on each electrode in full cell at different stages during cycling, which is important to deepen our knowledge of additive and provide new opportunities for the design of rational amount of additive according to the actual conditions. However, due to the lack of advanced technology, it is difficult to distinct where and how much

additive decomposes based on traditional characterizations such as X-ray photoelectron spectroscopy (XPS) and transmission electron microscope (TEM). Herein, we developed a new technique by combining the designed charge/discharge strategies and IC measurements to solve this issue, which is discussed below. Then, combined with traditional characterization methods such as XPS, TEM and time-of-flight secondary ion mass spectrum (TOF-SIMS) *etc.*, a comprehensive understanding of the effects of LiDFBOP additive on battery performance is deeply discussed.

3.3.1. Measurement of the continuous consumption of LiDFBOP additive on both electrodes simultaneously based on NMC622/SiO-C pouch cells by IC and controlled charging and discharging technique

Fig. 3a illustrates the process of method designed for quantitatively detecting the amount of LiDFBOP additive remaining in the electrolyte retrieved at different charging state of NMC622/SiO-C pouch cell. The specific testing details of IC is provided in the Experimental Section. As shown in Fig. 3b, two parallel NMC622/SiO-C pouch cells with LiDFBOP additive were prepared and one of them was charged to 4.3 V at a constant current density of 0.1C. During this formation process, the time spent was recorded as t2. Meanwhile, the other was only charged to 3.2 V at the same constant current density of 0.1C, the time spent of which was recorded as t1, and after which the cell was kept at constant voltage of 3.2 V until the total time spent was t2. According to the galvanostatic voltage profiles based on different battery configuration, the origin of voltage hysteresis in NMC622/SiO-C pouch cell can be confirmed by comparing to that happening in half cells. In details, when the pouch

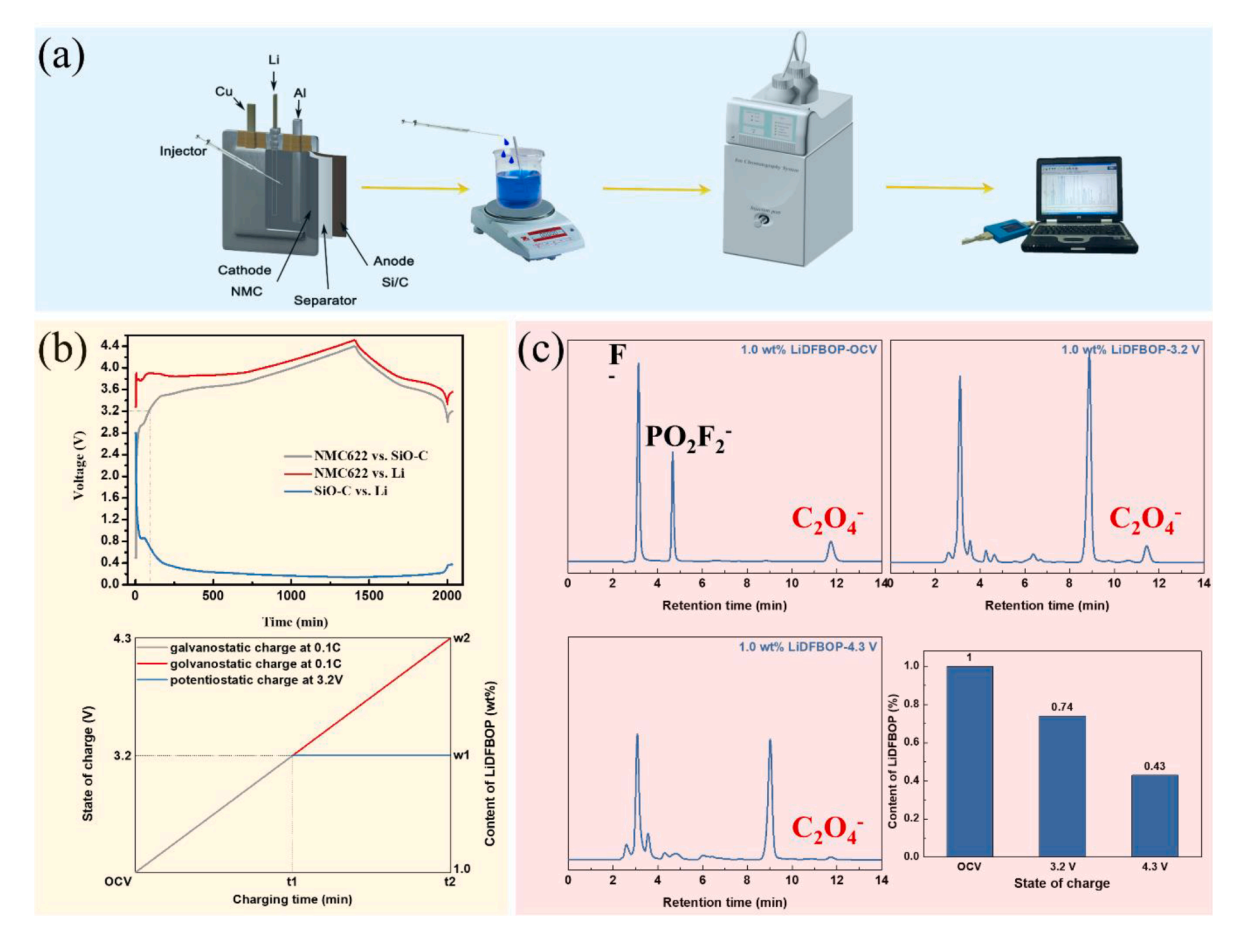


Fig. 3. Quantitatively analyzing the specific consumption amount of LiDFBOP additive simultaneously on each electrode in NMC622/SiO-C pouch cell. (a) Schematic of the process of analyzing the amount of LiDFBOP additive remaining in the electrolyte after cycling. (b) The galvanostatic voltage profiles of different battery configuration at the current density of 0.1C and the illustration of the amount of LiDFBOP additive remaining in the electrolyte associated to different charging state of pouch cell. (c) The IC spectra of electrolytes in the pouch cells at different charging state comparing and summarizing the contents of LiDFBOP additive remaining in the related electrolytes.

cells were charged to 3.2 V, the voltage change of which mainly depends on the polarization of negative electrode while almost unchanged in the potential of positive electrode, in which the oxidation decomposition of electrolyte on the cathode interfaces was negligible. As indicated in previous conclusions, since the reduction potential of LiDFBOP additive is 1.9 V (vs. Li metal), the consumption of LiDFBOP additive during this process mainly derived from its reduction decomposition on the surface of negative electrode. When the pouch cells were sequentially charged to 4.3 V, the voltage change of which mainly depend on the polarization of positive electrode as the potential of negative electrode tends to be constant, oxidation decomposition of electrolyte started and part of the consumption of LiDFBOP additive would occur on the cathode interfaces. Therefore, the amount of LiDFBOP additive consumed on the negative electrode in the latter pouch cell after cycling for t2 equals to that consumed throughout in the former one. The remaining amounts of LiDFBOP additive of these two pouch cells after cycling for t2 are denoted as w1 and w2 respectively, the difference between which is the consumption amount of LiDFBOP additive oxidizing on the positive electrolyte. The amount of LiDFBOP additive remaining in the electrolyte after cycled to different state of charging was quantitatively detected by IC technique. As shown in Fig. 3c, all the spectra have a characteristic peak of LiDFBOP, the intensity of which was fitted and normalized. When charged to 3.2 V and potentiostatically kept for t2, the value of w1 is 0.74 wt.%, indicating there is 0.26 wt.% LiDFBOP additive involved to construct the interface films on anode (SEIs) by its reduction decomposition. When directly charged to 4.3 V for t2, the value of w2 is 0.43 wt.%, indicating there is 0.31 wt.% (equals to w1w2) LiDFBOP additive involved in the formation of the interface films on cathode (CEIs) by its oxidation decomposition. Therefore, the method proposed here provides us a direct evidence that the LiDFBOP additive could decompose to help form a protective layer on both cathode and anode surfaces simultaneously. The detailed insight gained here sets up a new way of thinking to understand the consumption distribution of additive and regulate its usage amount based on different charging and discharging strategies to get a better performance and cost-saving batteries.

3.3.2. Characterization of the CEI layer on stablizing the NMC622 cathode In addition to the interface stability, the microstructural stability of NMC622 cathode is another key factor to influence its electrochemical stability. First of all, to confirm the effects of interface films formed in the LiDFBOP-containing electrolyte on the microstructural stability of NMC622 cathode, X-ray diffraction (XRD) patterns were acquired after 200 cycles as shown in Fig. S6. The corresponding lattice parameters were calculated and concluded in Table S4. In comparison with NMC622 cathode cycled in the baseline electrolyte, there is no noticeable change in that cycled in the LiDFBOP-added electrolyte, indicating the highly stable structure of the NMC cathode used in this research even after long-term cycling. Therefore, the improvement in electrochemical performance observed for the pouch cells with LiDFBOP-added electrolyte has a different origin, which could be due to the better CEI layers formed on the cathode surfaces, modifying interface Li+ dynamics, suppressing excessive decomposition of bulk electrolyte and improving their selfstability as discussed above.

To further verify this hypothesis, a series of characterizations were carried out aiming at dissecting the morphology, structure and composition on cathode surface under the participation of LiDFBOP additive. To detect the evolution of surface morphology of the NMC622 cathodes under different electrolytes after 400 cycles, the respective scanning electron microscopy (SEM) images are compared in Fig. S7. As observed in Fig. S7a-b, the fresh NMC622 cathode material comprises of secondary particles, which could be dispersed well and embraced by binder and conductive agent when preparing the NMC622 electrode. After cycled in the baseline electrolyte, it is clearly seen in Fig. S7c-d that the surface on the NMC622 cathode is covered with a layer of oxidation products and the particles of NMC622 show obvious tendency to break

into those with smaller sizes, suggesting that the protective layer formed without additive is in poor conditions of stability, homogeneousness and compactness. This film is unable to inhibit further oxidation decomposition of electrolyte, leading to the excessive corrosion towards bulk cathode materials during long-term cycling and final structural pulverization. Therefore, there occurs increasing resistance and deteriorated stability during cycling in the NMC622-based pouch cells using the baseline electrolyte. With the addition of 1.0 wt.% LiDFBOP to the baseline electrolyte, an integrated, homogeneous, compact and thin surface deposition layer covers the cathode surface as shown in Fig. S7ef, which is beneficial for fast Li+ migration and decreasing interfacial resistance, leading to the improved electrochemical performance as observed above. It can be concluded that LiDFBOP additive begins to decompose by oxidation at the formation stage and helps form a homogeneous and compact surface film on the cathode subsequently, thus effectively inhibiting the continuous oxidation decomposition of electrolyte, contributing to the structural integrity and improved cyclic stability of cathode material. To further understand the microstructure and thickness of surface layer on NMC622 cathode under different electrolytes, TEM was conducted. As shown in Fig. S8a, it is obvious to distinguish the boundary of pristine NMC622 particle without any coating layer attached. After cycled in the baseline electrolyte, as displayed in Fig. S8b, the NMC622 particle is coated with fragmented and uneven deposits, which might be caused by the dissolution of most of esterified organic macromolecules products. From the inset of selected area electron diffraction (SAED) pattern, the surface film mainly comprises of amorphous substance from the oxidation of solvents and a small amount of LiF and LixPOvFz from the oxidation of Li salts. After adding LiDFBOP additive to the baseline electrolyte, as exhibited in Fig. 4a, a uniform and compact protective layer is found to form on the cathode surface with the thickness of about 10 nm. From the inset of SAED pattern, with the effects of LiDFBOP, the surface film is rich in crystalline inorganic substance, leading to its excellent structural and electrochemical stability for suppressing the degradation of cathode material by preventing persistent attack from electrolyte.

Then XPS analysis [41], as a semi-quantitative surface-sensitivity method, was used to be carried out to further characterize the chemical compositions of the respective CEIs formed on the cathode surfaces in different electrolyte systems. To exclude the interference of decomposition of LiPF₆ salt and focus on the analysis of final LiDFBOP-derived CEIs, the lithium perchlorate (LiClO₄) was used as the electrolytic salt and 2 wt% LiDFBOP additive was introduced into the electrolyte. The probing depth is about 10 nm dependent on the applied experimental conditions. As shown in Fig. 4b, for the C 1s spectra from the cycled NMC622 electrode in LiDFBOP-added LiClO₄ salt-based electrolyte, there are five peaks centered in 284.4, 286.0, 288.6, 289.5 and 290.4 eV, corresponding to C-C sp2 hybridization bonds of conductive agent, C-O-C, -CO2 and -CO3 bonds of -CH2CH2Osemi-polycarbonate and trace amount of Li₂CO₃ products from decomposition of electrolyte, and C-F bonds of PVDF binder respectively. This suggests that the CEI layer covered on the NMC622 cathode is thin enough so that the signal from the bottom electrode can be also detected. As shown in Fig. S9, for the C 1s spectrum from the NMC622 cathode cycled in the baseline electrolyte, the peak at 289.5 eV representing -CO₃ bonds shows increasing relative intensity while the peak at 290.4 eV corresponding to C-F bonds of PVDF binder shows decreasing relative intensity than those from the fresh NMC622 cathode and the NMC622 cathode cycled in LiDFBOP-added electrolyte in Fig. 4b, demonstrating that the surface of the electrode cycled in the baseline electrolyte is abundant and covered with more Li₂CO₃ etc. by-products, which mainly originates from the excessive decomposition of carbonate solvents. The presence of many decomposition segments such as carbonyl groups leads to thicker interface layers with low ionic conductivity, brittleness and lack of adhesion with the underlying cathode surface, which can hardly protect NMC622 electrode from continuously attacked by electrolyte. To further confirm the participation of LiDFBOP additive in the

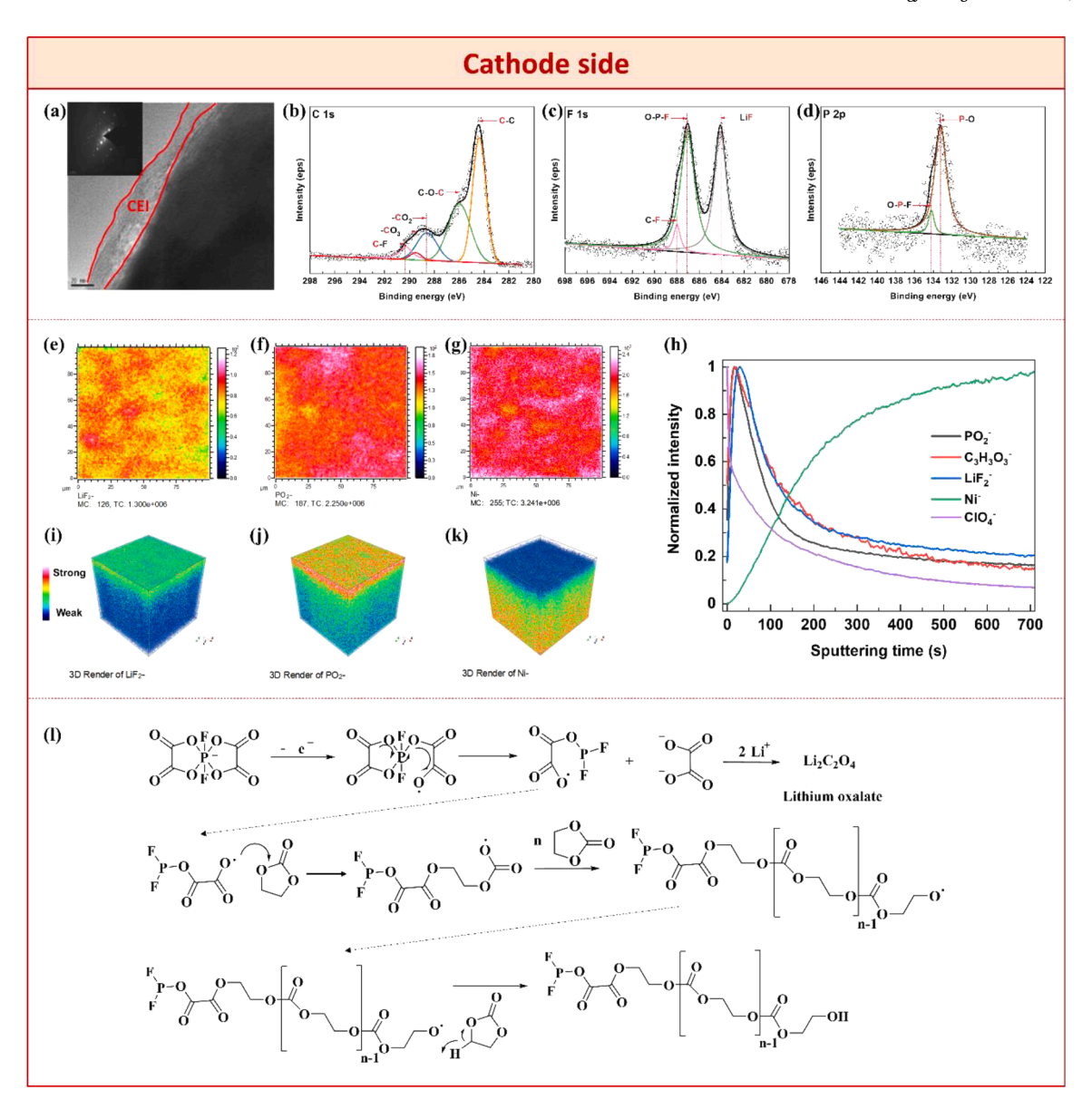


Fig. 4. The comprehensive characterizations of LiDFBOP additive-derived CEIs. (a) TEM and SAED images of NMC622 cathode cycled in the 1.0 wt% LiDFBOP-added electrolyte after 400 cycles. (b-d) XPS profiles of NMC622 cathode cycled in the 2.0 wt% LiDFBOP-added electrolyte with LiClO₄ as Li salt at 3rd half-charging state. (e-k) TOF-SIMS chemical maps (e-g), depth profiles (h), and corresponding 3D distributions (i-k) on NMC622 cathode harvested from 3-cycle pouch cells with LiClO₄ as Li salt and 2.0 wt% LiDFBOP additive. (l) Mechanism for the formation of LiDFBOP-involved CEIs.

formation of CEIs on NMC622 electrode, the F 1s and P 2p spectra were also acquired to help understand its possible decomposition process. For the F 1s spectrum of the CEI layer as shown in Fig. 4c, the presence of the peak of LiF directly indicates that LiDFBOP decompose to help form a more stable interface on cathode side, which can also be confirmed in the P 2p spectrum of the CEI layer as shown in Fig. 4d where a peak centered at 133.2 eV corresponding to the P-O group is clearly found, suggesting the break of P-F bonds in LiDFBOP. To further analyze the origin of this thin CEI film affected by the oxidation decomposition of LiDFBOP additive in the electrolyte, time-of-flight secondary ion mass spectrum (TOF-SIMS) chemical maps of different fragment ions were acquired on NMC622 cathode harvested from 3-cycle pouch cells with 2 wt% LiDFBOP additive. Fig.s 4e-k show the selected secondary ions maps and depth profiles on the cathode surface, and the corresponding 3D distributions. As shown in Fig. 4e-g, there shows strong LiF₂ and PO₂ signals uniformly distributing the surface of detected NMC622 cathode, which represent LiDFBOP-derived F-containing and P-containing decomposition products respectively, implying that LiDFBOP additive predominantly contributes to the construction of a high-quality CEI with more inorganic species. As displayed in Fig. 4h, the intensity of LiF₂ and PO₂ fragments quickly diminish during sputtering while the intensity of Ni⁻ fragments gradually increases during sputtering, indicating that LiDFBOP decomposition products reside on the surface of NMC622 cathode. This is visualized by the 3D-rendering view of LiF₂, PO₂, and Ni fragments in Fig. 4i-k. These observations well explain the formation of a uniform, dense and electrochemically stable CEI film with low resistance as discussed in TEM and EIS, which is regulated by the addition of LiDFBOP additive. As further understood with theoretical calculations, the formation mechanism of CEIs from the oxidation of LiDFBOP could be illustrated in Fig. 41 [32,42]. Therefore, it is reasonable to make a conclusion that the decomposition products of LiDFBOP, such as LiF and F-P-O macromoleclar polymer, help stabilize the high-voltage cathode interfaces, prevent the excessive oxidation decomposition of bulk electrolyte during long-term cycling, and promote interfacial dynamics, contributing to an improved electrochemical performance.

3.3.3. Characterization of the SEI layer on stablizing the SiO-C composite anode

As discussed above, in addition to preferential oxidation decomposition on the NMC622 cathode surfaces to help form a stable CEI layer, LiDFBOP is also expected to reduce preferentially on the SiO-C composite anode surfaces to help construct a protective SEI layer due to its lowest LUMO energy when compared to other components in the electrolyte. To further confirm this perspective and deeply understand the effects of LiDFBOP additive on the electrochemical performance of SiO-C composite anode, a series of characterizations were also conducted based on the anode side. SEM images of SiO-C composite anodes after different treatment are shown in Fig. S10. The particles of pristine composite anode material are angular and integrated. After cycling in the baseline electrolyte for 400 cycles, the surfaces of pristine composite particles are coated by a random stack of deposition layers with wide-spread product particles deriving from the reduction decomposition of electrolyte. As obtained from energy dispersive X-ray spectrum (EDS) in

Fig. S11a, these SEI films mainly comprise of C and O species with less F and P species, which might be from LiF and $\rm Li_x PO_y F_z$ produced by the decomposition of LiPF6, implying that organic species dominate the construction of SEIs in the baseline electrolyte. When adding the LiDFBOP additive to the baseline electrolyte, there is the integrated, thin, uniform and compact SEI films coating on the surface of SiO-C composite particles after 400 cycles, the composition of which mainly contains C species with small amount of P species from EDS in Fig. S11b, suggesting that the introduction of LiDFBOP contributes to suppress the excessive decomposition of Li salts.

Then the microstructure and thickness of surface films formed in different electrolytes were further detected at 100% state of charge (SOC) of SiO-C composites by TEM after 400 cycles. As shown in Fig. S12a, there is a clean interface on the fresh SiO-C electrode without any coating found. After long-term cycling in the baseline electrolyte, as depicted in Fig. S12b, a uneven and loose surface film with the thickness of 10-20 nm formed on the SiO-C composite electrode. In a sharp

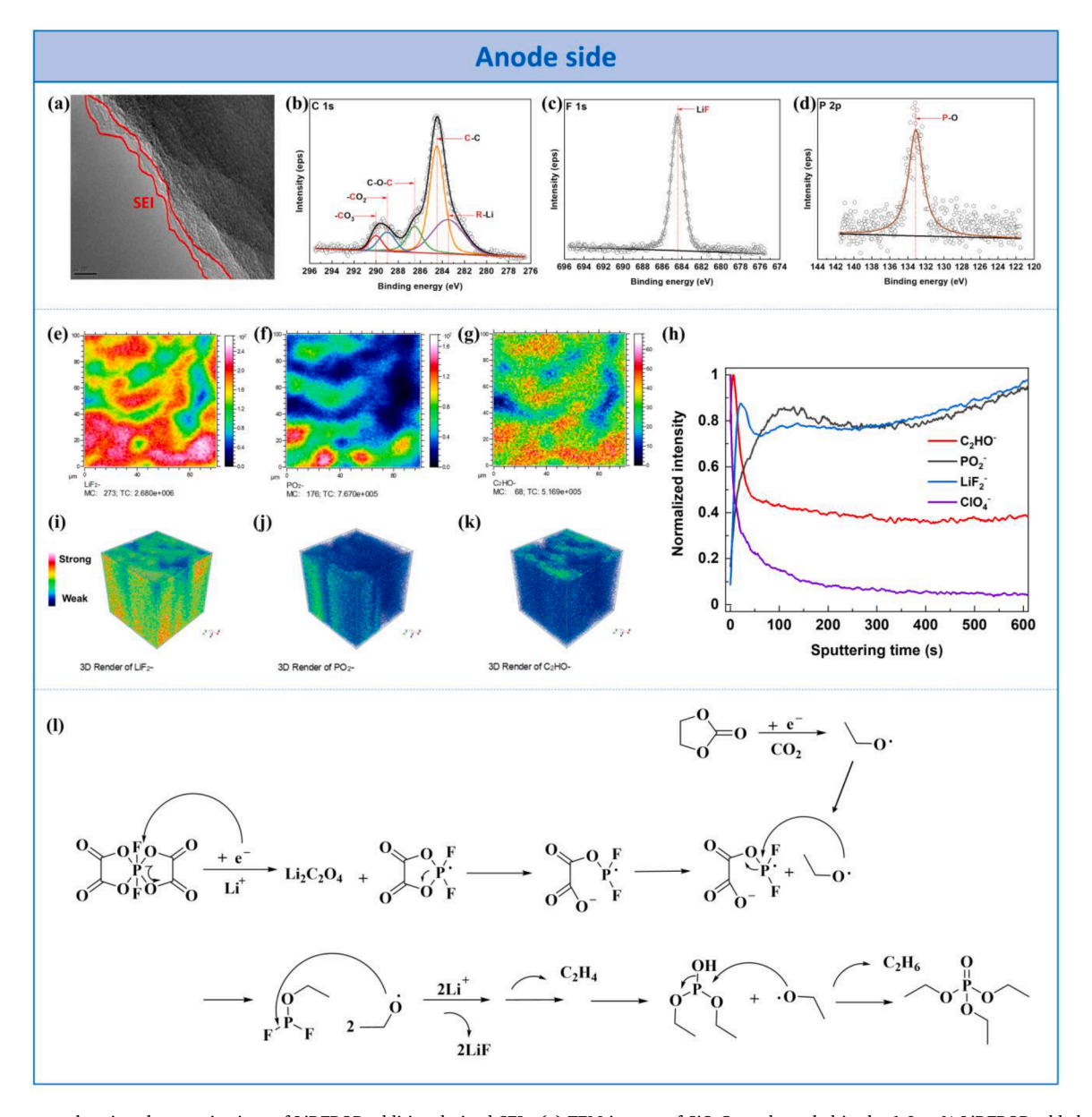


Fig. 5. The comprehensive characterizations of LiDFBOP additive-derived SEIs. (a) TEM images of SiO-C anode cycled in the 1.0 wt% LiDFBOP-added electrolyte after 400 cycles. (b-d) XPS profiles of SiO-C anode cycled in the 2.0 wt% LiDFBOP-added electrolyte with LiClO₄ as Li salt at 3rd half-charging state. (e-k) TOF-SIMS chemical maps (e-g), depth profiles (h), and corresponding 3D distributions (i-k) on SiO-C anode harvested from 3-cycle pouch cells with LiClO₄ as Li salt and 2.0 wt % LiDFBOP additive. (l) Mechanism for the formation of LiDFBOP-involved SEIs.

contrast, as exhibited in Fig. 5a, the presence of LiDFBOP additive in the electrolyte help regulate deposits on the anode interfaces, leading to a thin, uniform and dense SEI layer with the thickness of 3-5 nm, which well protects the anode from further corrosion by bulk electrolyte with its highly stable property and improves the ionic dynamics through interface. This is responsible for the improved cycling stability and rate capability as discussed above.

Except regulating the microstructure of interface layers on SiO-C composites, the LiDFBOP additive to the baseline electrolyte is expected to participate in the formation of SEIs and change their compositions, leading to different physicochemical properties and electrochemical behaviors, which can be verified by XPS measurements. As the same indicated above, LiClO₄ instead of LiPF₆ was used as electrolyte salt to exclude its influence on analyzing LiDFBOP-derived compositions in SEIs. As shown in Fig. 5b, for the C 1s spectrum harvested from the cycled SiO-C composite anode, there are five peaks emerging at 283.3, 284.5, 286.5, 289.0 and 290.0 eV due to the deposition of the products from electrolyte decomposition, assigned to lithium alkylide, C-C bonds corresponding to graphite, ether linkages, lithium alkyl carbonate and Li₂CO₃, respectively. For comparisons, the C 1s spectra from the pristine SiO-C electrode and the SiO-C electrode cycled in baseline electrolyte are also shown in Fig. S13. There are more -CO₃ species detected from the SiO-C anode cycled in the baseline electrolyte, which derive from the continuous decomposition of carbonate solvents due to the quite instable interfaces formed. This further suggests that the LiDFBOP-derived interface films are more capable to resist the constant volume change of bulk SiO-C anode during cycling. For the F 1s spectrum in Fig. 5c, there only exists one peaks centered at 684.5 eV, which can be assigned to LiF. This directly demonstrates the participation of LiDFBOP in the formation of SEIs by reduction decomposition. Interestingly, there is no any O-P-F bonds found, which can be also confirmed with only one peak found at 133.1 eV of P-O bond in the P 2p spectrum as shown in Figure 5d. This seems to suggest that the P-F bonds in LiDFBOP additive is more active towards reduction on anode side than oxidation on cathode side, finally leading to more LiF and P-O species participating in constructing an inorganic species-dominant, more stable and Li-conductive SEIs on anode side. TOF-SIMS was also used to further confirm the LiDFBOP-derived SEIs. As shown in Fig. 5e-k, strong signals from the decomposition products of LiF₂ and PO₂ are obviously detected and occupy the entire 3D-rendering space, indicating the reduction decomposition of LiDFBOP additive on the surface of SiO-C anode, which is in accordance with the results from XPS. In contrast, the C₂HO⁻ fragments, standing for EC/EMC solvents/oxalate anions reduction products, only reside on the very surface of SEIs. This points out that the formation of high-quality SEIs mainly tuned by LiDFBOP additive protects the SiO-C anode from severe electrolyte reduction side reactions. As further understood with theoretical calculations, the formation mechanism of SEIs from the reduction of LiDFBOP could be illustrated in Fig. 5l. Therefore, in a brief summary, the LiDFBOP additive helps form a composite surface film abundant with Li-containing fluorinated organic and inorganic species such as LiF and P-O compounds on the anode interface, which is thinner, more uniform and Li+ conductive than that formed in the baseline electrolyte, contributing to enhanced electrochemical stability of SEIs, fast Li⁺ diffusion through the interface and decreasing interfacial resistance, finally resulting in significantly improved rate capability and low-temperature performance.

4. Conclusion

In summary, we introduce a novel multifunctional additive, lithium difluorobis(oxalato) phosphate (LiDFBOP), to synchronously modulate the cathode/anode interfaces and improve the cycling stability of NMC622/SiO-C pouch cells. DFT calculations together with the electrochemical measurements manifest that LiDFBOP additive preferentially decomposes on both interfaces of cathode and anode, which

influences the subsequent electrochemical behaviors of bulk electrolyte, resulting in protective interface films and improving the cycling stability of battery. As expected, the NMC622/SiO-C pouch cells exhibit exceptional electrochemical performance with a superior capacity retention of 87.2% and high average CE exceeding 99.8% at a current rate of 1C after 400 cycles, much higher than that with the baseline electrolyte, even using LiBOB additive. The underlying film-forming mechanisms on cathode and anode are studied by complementary spectroscopic characterizations techniques. Thin, dense and ionically conductive interface films composed of Li-containing organic and inorganic species synchronously form on both sides of NMC622 cathode and SiO-C anode, stabilizing the electrodes interfaces and suppressing the excessive decomposition of the electrolyte, alleviating the dissolution of transition metal ions and expediting Li+ redox kinetics, thus in turn improving long-term cycling stability, rate capability as well as low-temperature performance of the pouch cells. Besides, a new method is proposed to quantitatively understand the consumption distribution of additive on each electrode in pouch cell based on the combination of designed charge/discharge strategies and IC measurements. The results show that timely regulation of interfacial layer and a usage amount of the additive in the electrolyte is very important for getting a better performance and cost-saving electrolyte for high-energy batteries. Overall, our work demonstrates the critical role of LiDFBOP additive on stablizing the interfaces on both cathode and anode simultaneously, and detailed insights gained provide a facile solution to develop surface-engineered electrode for realizing high energy and better performance lithium-ion batteries even operated at low temperature.

Author contributions

W. Zhao and G. Zheng contributed equally to this work. W. Zhao and G. Zheng designed the research. F. Pan and Y. Yang supervised the project. W. Zhao, G. Zheng, and Y. Ji prepared all the samples for testing, did the electrochemical measurements, the SEM/TEM observation and the spectroscopic studies (IC, XPS and TOF-SIMS *etc.*), and analysed the data. F. Ren conducted the theoretical simulations and helped analyse the related data. W. Zhao, G. Zheng, C. Peng and M. Liu contributed to the discussion of results. G. Zheng wrote the manuscript. W. Zhao, C. Peng, M. Liu, F. Pan and Y. Yang helped revise the manuscript.

Declaration of Competing Interest

The authors declare no competing financial interest.

Data availability

Data will be made available on request.

Acknowledgments

This work was financially supported by Shandong Provincial Natural Science Foundation (Grant No. ZR202011050003), National Key Research and Development Program of China (Grant No. 2018YFB0905400), National Natural Science Foundation of China (Grant Nos. 21761132030, 21621091 and 21473148), Soft Science Research Project of Guangdong Province (Grant No. 2017B030301013), and Major Science and Technology Infrastructure Project of Material Genome Big-science Facilities Platform supported by Municipal Development and Reform Commission of Shenzhen. Weimin Zhao and Guorui Zheng contributed equally to this work.

Supplementary materials

Supplementary material associated with this article can be found, in the online version, at doi:10.1016/j.ensm.2022.09.024.

References

- [1] X. Fan, C. Wang, High-voltage liquid electrolytes for Li batteries: progress and perspectives, Chem. Soc. Rev. 50 (2021) 10486.
- [2] J. Hu, Y. Ji, G. Zheng, W. Huang, Y. Lin, L. Yang, F. Pan, Influence of electrolyte structural evolution on battery applications: Cationic aggregation from dilute to high concentration, Aggregate 3 (2022) e153.
- [3] M. Li, J. Lu, Z. Chen, K. Amine, 30 Years of Lithium-Ion Batteries, Adv. Mater. 30 (2018), e1800561.
- [4] M. Winter, B. Barnett, K. Xu, Before Li Ion Batteries, Chem. Rev. 118 (2018) 11433.
- [5] Z. Yin, J. Li, L. Huang, F. Pan, S. Sun, High-capacity Li-rich Mn-based Cathodes for Lithium-ion Batteries, Chin. J. Struct. Chem. 39 (2020) 20.
- [6] A. Manthiram, J.C. Knight, S.T. Myung, S.M. Oh, Y.K. Sun, Nickel-Rich and Lithium-Rich Layered Oxide Cathodes: Progress and Perspectives, Adv. Energy Mater. 6 (2016), 1501010.
- [7] M.M. Thackeray, K. Amine, Layered Li-Ni-Mn-Co oxide cathodes, Nat. Energy 6 (2021) 933.
- [8] F. Cheng, X. Zhang, Y. Qiu, J. Zhang, Y. Liu, P. Wei, M. Ou, S. Sun, Y. Xu, Q. Li, C. Fang, J. Han, Y. Huang, Tailoring electrolyte to enable high-rate and superstable Ni-rich NCM cathode materials for Li-ion batteries, Nano Energy 88 (2021), 106301.
- [9] X. Fan, X. Ou, W. Zhao, Y. Liu, B. Zhang, J. Zhang, L. Zou, L. Seidl, Y. Li, G. Hu, C. Battaglia, Y. Yang, In situ inorganic conductive network formation in highvoltage single-crystal Ni-rich cathodes, Nat. Commun. 12 (2021) 5320.
- [10] Z. Cui, Q. Xie, A. Manthiram, A Cobalt- and Manganese-Free High-Nickel Layered Oxide Cathode for Long-Life, Safer Lithium-Ion Batteries, Adv. Energy Mater. 11 (2021), 2102421.
- [11] J. Zheng, Y. Ye, T. Liu, Y. Xiao, C. Wang, F. Wang, F. Pan, Ni/Li Disordering in Layered Transition Metal Oxide: Electrochemical Impact, Origin, and Control, Acc. Chem. Res. 52 (2019) 2201.
- [12] Y.M. Lee, K.M. Nam, E.H. Hwang, Y.G. Kwon, D.H. Kang, S.S. Kim, S.W. Song, Interfacial Origin of Performance Improvement and Fade for 4.6 V LiNi_{0.5}Co_{0.2}Mn_{0.3}O₂ Battery Cathodes, J. Phys. Chem. C 118 (2014) 10631.
- [13] Y. Wu, X. Liu, L. Wang, X. Feng, D. Ren, Y. Li, X. Rui, Y. Wang, X. Han, G.L. Xu, H. Wang, L. Lu, X. He, K. Amine, M. Ouyang, Development of cathode-electrolyte-interphase for safer lithium batteries, Energy Storage Mater. 37 (2021) 77.
- [14] Y. Yang, J. Yang, F. Pan, Y. Cui, From Intercalation to Alloying Chemistry: Structural Design of Silicon Anodes for the Next Generation of Lithium-ion Batteries, Chin. J. Struct. Chem. 39 (2020) 16.
- [15] J.D. McBrayer, M.T.F. Rodrigues, M.C. Schulze, D.P. Abraham, C.A. Apblett, I. Bloom, G.M. Carroll, A.M. Colclasure, C. Fang, K.L. Harrison, G. Liu, S. D. Minteer, N.R. Neale, G.M. Veith, C.S. Johnson, J.T. Vaughey, A.K. Burrell, B. Cunningham, Calendar aging of silicon-containing batteries, Nat. Energy 6 (2021) 866.
- [16] G. Zheng, Y. Xiang, L. Xu, H. Luo, B. Wang, Y. Liu, X. Han, W. Zhao, S. Chen, H. Chen, Q. Zhang, T. Zhu, Y. Yang, Controlling Surface Oxides in Si/C Nanocomposite Anodes for High-Performance Li-Ion Batteries, Adv. Energy Mater. 8 (2018), 1801718.
- [17] B. Zhu, X. Wang, P. Yao, J. Li, J. Zhu, Towards high energy density lithium battery anodes: silicon and lithium, Chem. Sci. 10 (2019) 7132.
- [18] K. Xu, Electrolytes and Interphases in Li-Ion Batteries and Beyond, Chem. Rev. 114 (2014) 11503.
- [19] A.M. Haregewoin, A.S. Wotango, B.-J. Hwang, Electrolyte additives for lithium ion battery electrodes: progress and perspectives, Energy Environ. Sci. 9 (2016) 1955.
- [20] X. Yang, M. Lin, G. Zheng, J. Wu, X. Wang, F. Ren, W. Zhang, Y. Liao, W. Zhao, Z. Zhang, N. Xu, W. Yang, Y. Yang, Enabling Stable High-Voltage LiCoO₂ Operation by Using Synergetic Interfacial Modification Strategy, Adv. Funct. Mater. 30 (2020), 2004664.
- [21] Q. Zheng, G. Li, X. Zheng, L. Xing, K. Xu, W. Li, Sulfolane-Graphite Incompatibility and Its Mitigation in Li-ion Batteries, Energy Environ. Mater. 0 (2021) 1.
- [22] L. Fu, X. Wang, L. Wang, M. Wan, Y. Li, Z. Cai, Y. Tan, G. Li, R. Zhan, Z.W. Seh, Y. Sun, A Salt-in-Metal Anode: Stabilizing the Solid Electrolyte Interphase to Enable Prolonged Battery Cycling, Adv. Funct. Mater. 31 (2021), 2010602.
- [23] N. Piao, S. Liu, B. Zhang, X. Ji, X. Fan, L. Wang, P.-F. Wang, T. Jin, S.C. Liou, H. Yang, J. Jiang, K. Xu, M.A. Schroeder, X. He, C. Wang, Lithium Metal Batteries

- Enabled by Synergetic Additives in Commercial Carbonate Electrolytes, ACS Energy Lett. 6 (2021) 1839.
- [24] S. Klein, P. Harte, J. Henschel, P. Bärmann, K. Borzutzki, T. Beuse, S. Wickeren, B. Heidrich, J. Kasnatscheew, S. Nowak, M. Winter, T. Placke, On the Beneficial Impact of Li₂CO₃ as Electrolyte Additive in NCM523 || Graphite Lithium Ion Cells Under High-Voltage Conditions, Adv. Energy Mater. 11 (2021), 2003756.
- [25] J. Zheng, M.H. Engelhard, D. Mei, S. Jiao, B.J. Polzin, J.G. Zhang, W. Xu, Electrolyte additive enabled fast charging and stable cycling lithium metal batteries, Nat. Energy 2 (2017) 17012.
- [26] W. Zhao, G. Zheng, M. Lin, W. Zhao, D. Li, X. Guan, Y. Ji, G.F. Ortiz, Y. Yang, Toward a stable solid-electrolyte-interfaces on nickel-rich cathodes: LiPO₂F₂ salttype additive and its working mechanism for LiNi_{0.5}Mn_{0.25}Co_{0.25}O₂ cathodes, J. Power Sources 380 (2018) 149.
- [27] G. Zheng, Y. Xiang, S. Chen, S. Ganapathy, T.W. Verhallen, M. Liu, G. Zhong, J. Zhu, X. Han, W. Wang, W. Zhao, M. Wagemaker, Y. Yang, Additives synergy for stable interface formation on rechargeable lithium metal anodes, Energy Storage Mater. 29 (2020) 377.
- [28] K. Xu, S.S. Zhang, U. Lee, J.L. Allen, T.R. Jow, LiBOB: Is it an alternative salt for lithium ion chemistry? J. Power Sources 146 (2005) 79.
- [29] S.Y. Ha, J.G. Han, Y.M. Song, M.J. Chun, S.I. Han, W.C. Shin, N.S. Choi, Using a lithium bis(oxalato) borate additive to improve electrochemical performance of high-voltage spinel LiNi_{0.5}Mn_{1.5}O₄ cathodes at 60 °C, Electrochim. Acta 104 (2013) 170.
- [30] B. Liao, H. Li, M. Xu, L. Xing, Y. Liao, X. Ren, W. Fan, L. Yu, K. Xu, W. Li, Designing Low Impedance Interface Films Simultaneously on Anode and Cathode for High Energy Batteries, Adv. Energy Mater. 8 (2018), 1800802.
- [31] H. Ma, D. Hwang, Y.J. Ahn, M.Y. Lee, S. Kim, Y. Lee, S.M. Lee, S.K. Kwak, N. S. Choi, In Situ Interfacial Tuning To Obtain High-Performance Nickel-Rich Cathodes in Lithium Metal Batteries, ACS Appl. Mater. Interfaces 12 (2020) 29365.
- [32] G. Song, Z. Yi, F. Su, L. Xie, C. Chen, New Insights into the Mechanism of LiDFBOP for Improving the Low-Temperature Performance via the Rational Design of an Interphase on a Graphite Anode, ACS Appl. Mater. Interfaces 13 (2021) 40042.
- [33] N.P.W. Pieczonka, L. Yang, M.P. Balogh, B.R. Powell, K. Chemelewski, A. Manthiram, S.A. Krachkovskiy, G.R. Goward, M. Liu, J.H. Kim, Impact of Lithium Bis(oxalate)borate Electrolyte Additive on the Performance of High-Voltage Spinel/Graphite Li-Ion Batteries, J. Phys. Chem. C 117 (2013) 22603.
- [34] M. Li, J. Gu, X. Feng, H. He, C. Zeng, Amorphous-silicon@silicon oxide/chromium/ carbon as an anode for lithium-ion batteries with excellent cyclic stability, Electrochim. Acta 164 (2015) 163.
- [35] Y. Gu, W. Zhao, C. Su, C. Luo, Z. Zhang, X. Xue, Y. Yang, Research Progresses in Improvement for Low Temperature Performance of Lithium-Ion Batteries, J. Electrochem. 24 (2018) 488.
- [36] Q. Li, G. Liu, H. Cheng, Q. Sun, J. Zhang, J. Ming, Low-Temperature Electrolyte Design for Lithium-Ion Batteries: Prospect and Challenges, Chemistry 27 (2021) 15842.
- [37] N.-S. Choi, K.H. Yew, K.Y. Lee, M. Sung, H. Kim, S.S. Kim, Effect of fluoroethylene carbonate additive on interfacial properties of silicon thin-film electrode, J. Power Sources 161 (2006) 1254.
- [38] L. Chen, K. Wang, X. Xie, J. Xie, Effect of vinylene carbonate (VC) as electrolyte additive on electrochemical performance of Si film anode for lithium ion batteries, J. Power Sources 174 (2007) 538.
- [39] M. Xu, W. Li, B.L. Lucht, Effect of propane sultone on elevated temperature performance of anode and cathode materials in lithium-ion batteries, J. Power Sources 193 (2009) 804.
- [40] D. Xu, Y. Kang, J. Wang, S. Hu, Q. Shi, Z. Lu, D. He, Y. Zhao, Y. Qian, H. Lou, Y. Deng, Exploring synergetic effects of vinylene carbonate and 1,3-propane sultone on LiNi_{0.6}Mn_{0.2}Co_{0.2}O₂/graphite cells with excellent high-temperature performance, J. Power Sources 437 (2019), 226929.
- [41] P. Verma, P. Maire, P. Novak, A review of the features and analyses of the solid electrolyte interphase in Li-ion batteries, Electrochim. Acta 55 (2010) 6332.
- [42] J.-G. Han, I. Park, J. Cha, S. Park, S. Park, S. Myeong, W. Cho, S.S. Kim, S.Y. Hong, J. Cho, N.S. Choi, Interfacial Architectures Derived by Lithium Difluoro(bisoxalato) Phosphate for Lithium-Rich Cathodes with Superior Cycling Stability and Rate Capability, ChemElectroChem 4 (2017) 56.